Hindawi
Geofluids
Volume 2022, Article ID 7571371, 11 pages
https://doi.org/10.1155/2022/7571371

Research Article

Study on the Evolution Laws of Anchoring Property of Surrounding Rock of Argillaceous Weakly Cemented Roadway in Water Environment

Weiguang Zhang,[1,2] Zhiguo Chang,[3] Jianbiao Bai,[1,2] and Rui Wang[2]

[1]*Mining Engineering and Geology College, Xinjiang Institute of Engineering, Urumqi, Xinjiang 830023, China*
[2]*State Key Laboratory of Coal Resources and Safe Mining, School of Mines, China University of Mining & Technology, Xuzhou 221116, China*
[3]*School of Safety Science and Engineering, Xinjiang Institute of Engineering, Urumqi 830023, China*

Correspondence should be addressed to Zhiguo Chang; changzg@cumt.edu.cn and Jianbiao Bai; baijianbiao@cumt.edu.cn

Received 12 April 2022; Revised 18 May 2022; Accepted 28 May 2022; Published 27 June 2022

Academic Editor: Jinpeng Zhang

This paper is aimed at studying the influence of composition and microstructure on the Jurassic weakly cemented rock mechanical properties. No. 1802 tailentry was used as the engineering background, located in the Danan Lake No. 5 mine in Xinjiang, China. The weakly cemented sandstone compositions were analyzed by using X-ray diffraction instrument. And the microstructure was observed by using a scanning electron microscope. The uniaxial compression experiment was carried out to investigate the mechanical characteristics by using MTS mechanics experimental system, and the uniaxial compressive strength, Poisson's ratio, and elastic modulus were obtained. The relationships between the mechanical parameters that include the mineral composition, microstructural characteristics, uniaxial compressive strength (UCS), elastic modulus, cohesion, and friction angle of the weakly cemented sandstone and the water content were obtained. The attenuation of the anchorage force of the weakly cemented surrounding rock under different water-rich conditions was studied. The key reason of No. 1802 tailentry surrounding rock structure deterioration and roof fall was found. The model of a single anchor structure was established based on FLAC^{3D} to study the mechanical response of a single anchor structure under different water contents and the distribution and evolution laws of bearing stress field, effective compressive stress, and anchor axial force. The influences of parameters such as water content, pretightening force, and anchor length on the preload diffusion effect of weakly cemented surrounding rock anchorage structures are obtained. The key to controlling the deterioration of the surrounding rock structure of the weakly cemented entry is to reduce the water content of the roof. The research results provide reference for the control of the entry surrounding rock under similar stratum conditions.

1. Introduction

Many mining areas are dominated by Jurassic strata in Xinjiang, China, and the estimated amount of resources accounts for about 60% of Xinjiang coal resources, such as Shaer Lake Mining Area and Danan Lake Mining Area. Due to the diagenetic history, diagenetic environment, and sedimentary process of these types of strata, which are different from those of eastern China, they have the characteristics of high clay mineral content, high porosity, loose structure, and water sensitivity, which usually caused roof collapse accidents in those areas [1–4]. The scholars from various countries have taken up a lot of researches on the macrostructural characteristics and mechanical properties of weakly cemented rocks [5].

(1) Aspects of macrostructure: the hydration and disintegration characteristics and the reasons of mudstones are analyzed when they encounter water from the perspective of the element, crystalline

structure, and particle morphology using X-ray fluorescence spectrometer (XRF), X-ray diffractometer (XRD), and energy-dispersive X-ray analysis technology (EDAX) [6, 7]. The scanning electron microscopy, polarizing microscope, and X-ray diffraction are used to measure the water absorption, wetting angle, microscopic structure of mineral particles, changes in porosity during immersion in rocks, and the change law of microstructure of rock softening [8–10]. A large number of experimental studies have been conducted on the strength and failure characteristics of weakly cemented rock masses: whether it is a natural rock or a structurally restructured specimen, the experimental results with a single crack specimen show that the wing crack and the secondary crack will be derived from the crack tip under the axial loading [11]. The strength characteristics and failure characteristics of joint samples under confining pressure are analyzed, and three failure modes (single transfixion plane failure, stepped failure, and block rotation failure) are obtained [12]

(2) Numerical simulation aspects of rock deformation and failure: the failure characteristics of jointed and anisotropic rock masses are studied based on the RFPA2D software [13]. Munjiza [14] proposed a numerical calculation method combining the finite element and the discrete element. In this numerical calculation method, each finite element mesh has a corresponding discrete element. The continuous deformation of the rock mass under load is calculated using the finite element part, and the noncontinuous deformation is calculated using the discrete element part

(3) In deformation mechanism and control technology of surrounding rock of weakly cemented roadway respects: The elastic-plastic flow damage models of surrounding rock of weakly cemented soft rock roadway are established, and the influence of different factors on the stress, displacement, and plastic zone of the entry surrounding rock are studied [15–17]. The stress expansion factors of surrounding rock to characterize the effect of surrounding rock stress diffusion are defined, and the stress distribution and deformation failure characteristics of surrounding rock in the roadway of extremely weak cemented strata are revealed [18–22]. The secondary combined support of cable, net, and anchor support technology to large deformation and failure of weakly cemented soft rocks in the Yili area are proposed [23]. The optimal section and supporting measures for weakly cemented soft rock entry by analyzing the evolution law of surrounding rock stability under various roadway sections and supporting technologies are proposed [24]

Obviously, the research results are not mature on the interaction mechanism between the structural deterioration of weakly cemented surrounding rock and anchorage system under the water-rich condition roof. Therefore, this paper will analyze the reasons of roof falling accident of the No. 1802 tailentry and reveal the catastrophe and anchorage mechanism of the surrounding rock of weakly cemented entry at the Danan Lake Mine in Hami, Xinjiang, China.

2. Mining and Geological Conditions

2.1. Mining Specifications. The No. 5 mine field of the western part of Danan Lake is located in Hami City, Xinjiang Uygur Autonomous Region, China (Figure 1(a)). It belongs to the hydrogeological unit of the Danan Lake depression area. The northern part of the mine field is bounded by the F1 fault, the southern part is bounded by the hidden outcrop of the outermost coal seam, the western part is bounded by the eastern boundary of the exploration right of Luneng, and the eastern part is adjacent to the No. 6 mine field of Danan Lake. The mine field is 13.28 km long from east to west and 8.44 km-10.04 km wide from north to south, and the area is almost 105.70 km^2.

The No. 1802 panel is arranged in parallel with the No. 1801 panel. The selected panel is 2100 m long along the strike and 180 m wide along the dip. Top mining technology is adopted for the long wall mining. The No. 1802 panel is being prepared (Figure 1(b)). The depth of 18# coal seam is 225.5 m. The average thickness of 18# coal seam is 2.49 m. The dip of coal seam belongs to nearly horizontal coal seam. The immediate roof of the investigative entry is sandy mudstone and siltstone. This gritstone aquifer is close to the coal seam and is the main aquifer that affects mining. Gravel-bearing gritstone is generally present above the immediate roof. Although this aquifer will not cause large-scale water inflow in the mine, it will affect the stability of the surrounding rock of the entry.

2.2. The Engineering Problems. A roof falling accident occurred at 380 m in the No. 1802 tailentry. The boundary distance of the falling area was 4 m from heading face and 680 m from the adjacent panel (Figure 1(b)). The falling range was about 10 m, the entry width of the roof falling area was 4.3 m, and the falling height was 2.0 m-2.7 m. It shown that the coal seam and roof in the falling area are unconformity contacted, and lots of rocks with poor cementation, water softening, and low strength are scattered. The accumulation of the falling rocks was mostly wet soil and medium coarse gravel (Figure 2).

3. Cause Analysis for Roof Fall

Roof collapse, which is considered a significant hazard, refers to the drastic falling of rocks from roadway roofs, resulting in personal injuries and damage to equipment [25]. From 2004 to 2015, the total casualties in China caused by the roadway roof collapse accounted for 36.54%, resulting in a total of 12,689 deaths [26]. There are several factors that contribute to roadway roof collapse, including complicated geological conditions (such as faults, collapse pillars, and joints), inadequate reinforcement systems [27, 28], the weakening of rocks by the underground water, and weak

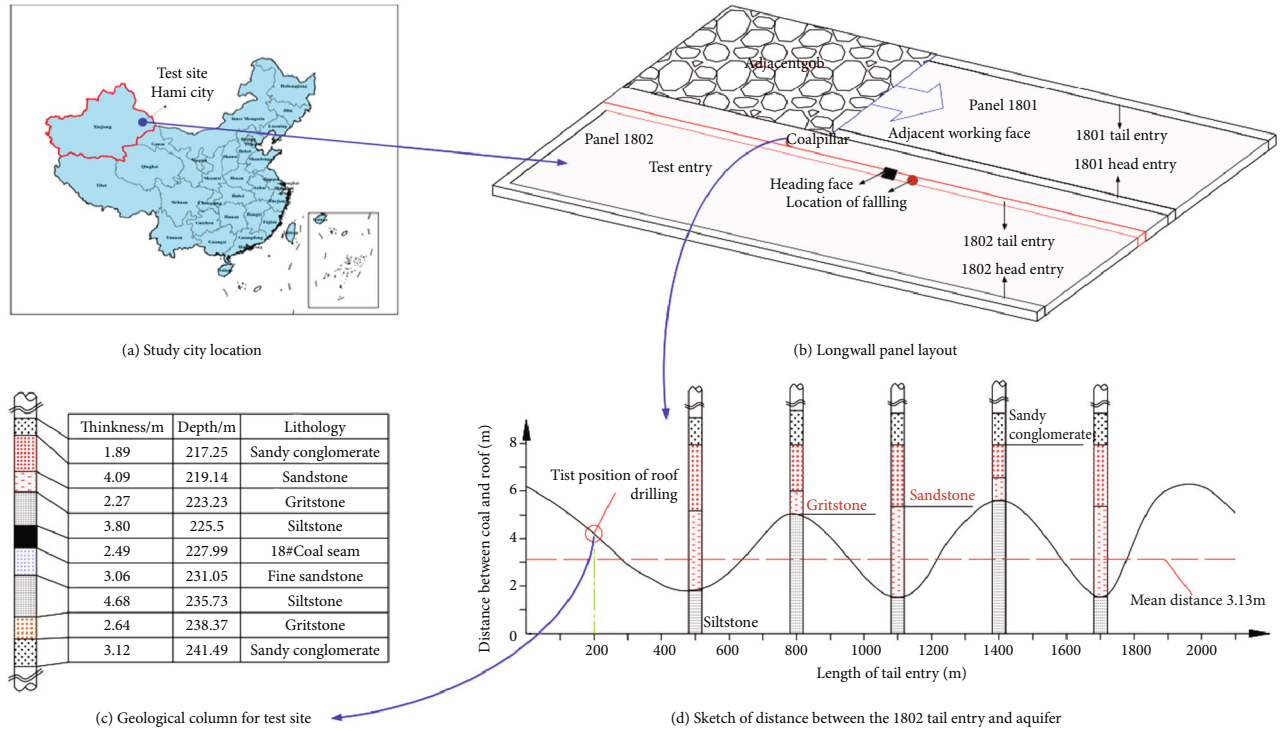

Figure 1: Location and generalized stratigraphic column of 1802 tailentry.

Figure 2: The morphological characteristics of falling rocks.

interlayers in the roof, as well as other mining factors. The previous research results [29, 30] show that the influence range of the advancing abutment pressure on the panel is 60 m-100 m. However, the location of the No. 1802 tailentry roof fall from the working face is 680 m, and the influence of mining can be ignored. Weakly cemented rocks are weakened by water, because water can cause deformation and structural damage of rocks. This rock failure is the main reason for the roof to be weakened by water, and it is related to the composition of the rock itself and the internal microstructure.

3.1. Analysis of Rock Composition and Microstructure. For microstructure research, the relationship between microstructure and rock mechanics properties has been analyzed [31–33]. In order to study the effect of rock composition, microstructure, and porosity on rock mechanics properties, the mineral composition and microstructure of the rock were selected for this research. Their compositions were analyzed by a D/Max-3BX-ray diffraction instrument. Composition analysis employed the X-ray diffractometer manufactured by Bruker Co. of Japan. One sample was made for composition and SEM analyses. The sample for composition analysis was ground to powder, while the SEM sample was made to a disk with a size of 0.5 cm ∗ 0.5 cm ∗ 0.5 cm. It can be seen from Figure 3 that the main components of the roof stratum are kaolinite and chlorite. Major minerals include kaolinite (33.1%), chlorite (21.6%), illite mixed layers (4.8%), illite (9.7%), montmorillonite (9.2%), and quartz (16.3%). Obviously, the water content of the rock increased after the high water content of kaolinite, and the montmorillonite and illite mixed layers undergo an intense expansion, eventually weakening the strength of the roof stratum.

The weakly cemented microstructure has a greater impact on the weakening of rock strength. Electron rays generated by a transmission electron microscope illuminate an object to improve its resolving power, and it can observe

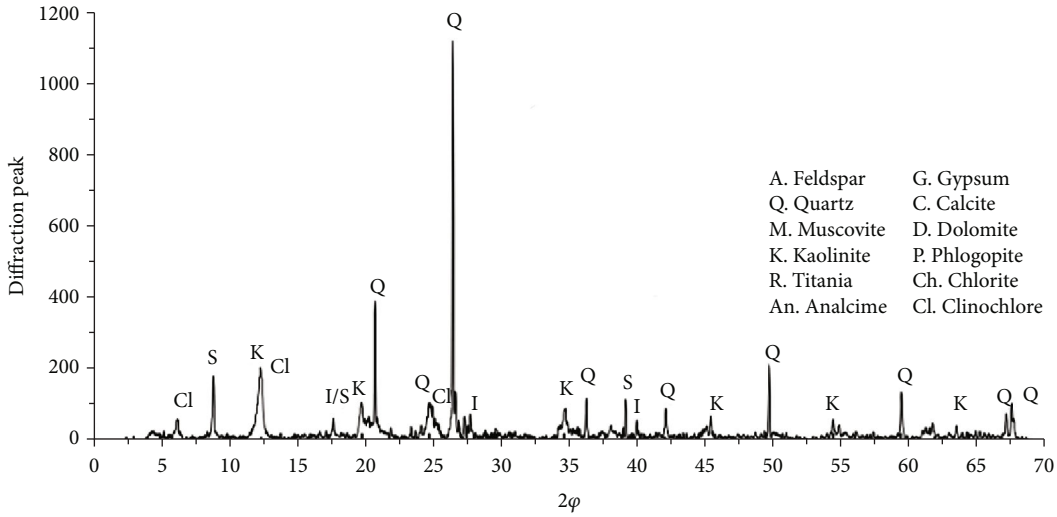

Figure 3: X-ray diffraction analysis of argillaceous weakly cemented rock.

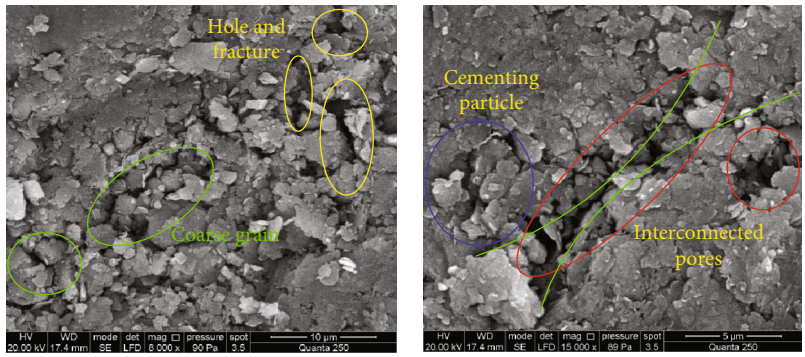

(a) Zoom in 8000 times (b) Zoom in 15000 times

Figure 4: Scanning electron microscope results of sandstones.

the microscopic morphology and structure of matter [34, 35]. The sandy mudstone of the No. 1802 tailentry roof was selected, and its microstructure was observed using a scanning electron microscope (SEM). Figure 4 shows the SEM photos for the sandy mudstone. It can be seen that there are many large coarse particles in the rock sample. The coarse particles are composed of small particles of clay minerals connected with each other or with coarse particles such as quartz and feldspar. The particles have poor cementation, irregular shapes and sizes, and numerous holes, and fractures are formed in the rock sample. These pores and fractures provide advantage conditions for water immersion. Clay minerals in rocks are easily swelling when interacting with water, which causes cracks inside the rocks to expand, leading to a decrease in roof strength.

3.2. Analysis of Rock Sensitivity to Water

3.2.1. Uniaxial Compression Experiment. Table 1 shows the results of uniaxial compressive strength (UCS), elastic modulus, Poisson's ratio, and water content. According to the results of uniaxial compression experiment, the relationships between the uniaxial compressive strength, elastic modulus, Poisson's ratio, and water content of the weakly cemented rock are fitted (Figure 5). As the water content of weakly cemented rocks increases, the uniaxial compressive strength and elastic modulus of the rocks is an exponential decay relation, but Poisson's ratio does not change significantly. The weakening effect of water on the strength of the weakly cemented rock stratum is obvious, revealing the deformation and instability reason under the water effect for the weak cemented water-rich entry surrounding rock.

3.2.2. Shear Experiments. In order to analyze the relationship between the cohesion, internal friction angle, and the water content of the weakly cemented rock, the rock samples with water content of 0%, 1.5%, 3.1%, and 5.7% were taken for shear tests. The relationships with cohesion, internal friction angle, and water content of the weakly cemented rock were obtained. As shown in Figure 6, the cohesion decreases linearly, the internal friction angle does not change obviously, and there is a slight increase after the water content of the weakly cemented rock increases, and the strength of the weakly cemented rock decreases with the action of water.

Table 1: The results of uniaxial compression experiment of weakly cemented rocks under different water content.

Rock samples	Water content (%)	Uniaxial compressive strength (MPa)	Elastic modulus (GPa)	Poisson's ratio (μ)
Sandy mudstone	0	19.2	3.92	0.25
	1.42	12.6	2.56	0.21
	2.91	8.7	1.87	0.27
	5.64	3.5	1.22	0.22
	7.75	1.3	0.56	0.23

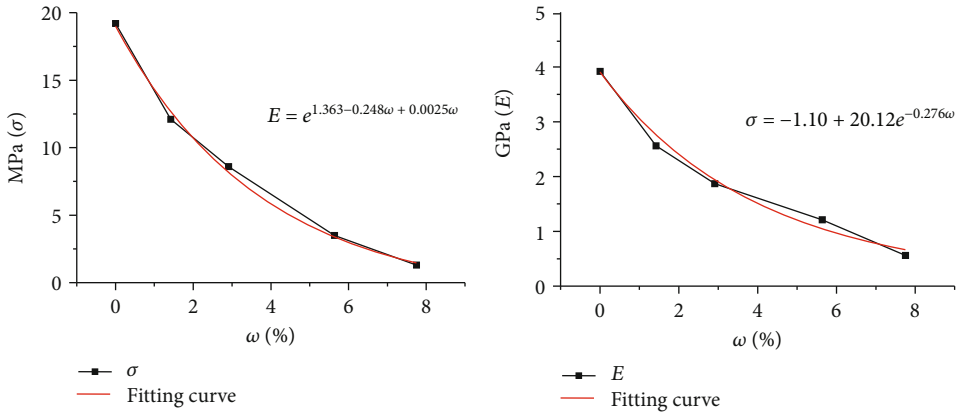

(a) σ-ω (b) E-ω

Figure 5: Fitting curve of σ-ω and E-ω about weakly cemented rock.

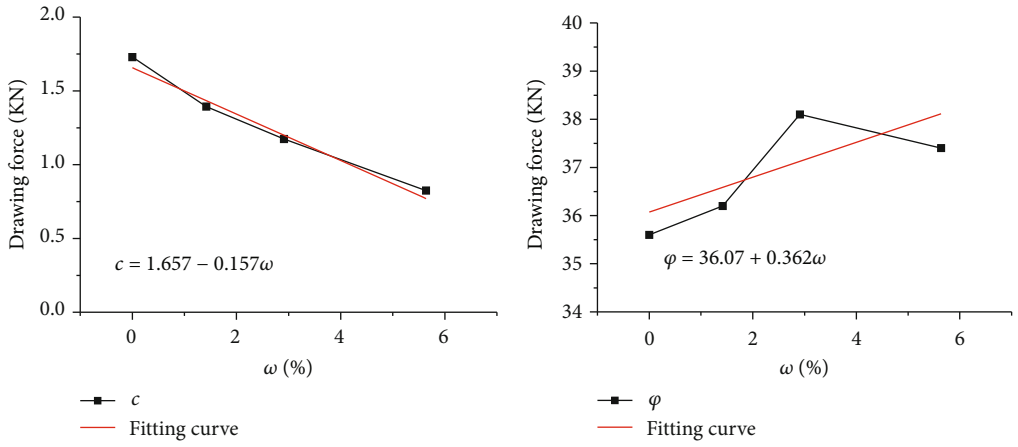

(a) c-ω (b) φ-ω

Figure 6: Fitting curve of c-ω and φ-ω about weakly cemented rock.

3.3. Anchorage Force Test of Gateway Surrounding Rock. According to the water content condition of the roof, No. 1 station (100 m~150 m), No. 2 station (180 m~220 m), and No. 3 station (250 m~320 m) are arranged in the 1802 tailentry, respectively. The aquifer at No. 1 station is high, and there is no water seepage on the roof. The No. 2 and No. 3 stations have a low aquifer, and the No. 3 station has a large amount of water seepage on the roof. As shown in Figure 7, the water content of the surrounding rock affects the anchorage force of the bolt. The anchorage force is negatively related to time. The anchorage force of the bolt decays rapidly with the increase of the time when the water content of surrounding rocks is high. The change in the water content of the surrounding rock under the aquifer layer has little effect on the drawing load of the anchor cable when the anchorage section of the anchor cable is located above the aquifer. However, when the anchorage section is in the aquifer layer, the drawing load of the anchor cable is reduced.

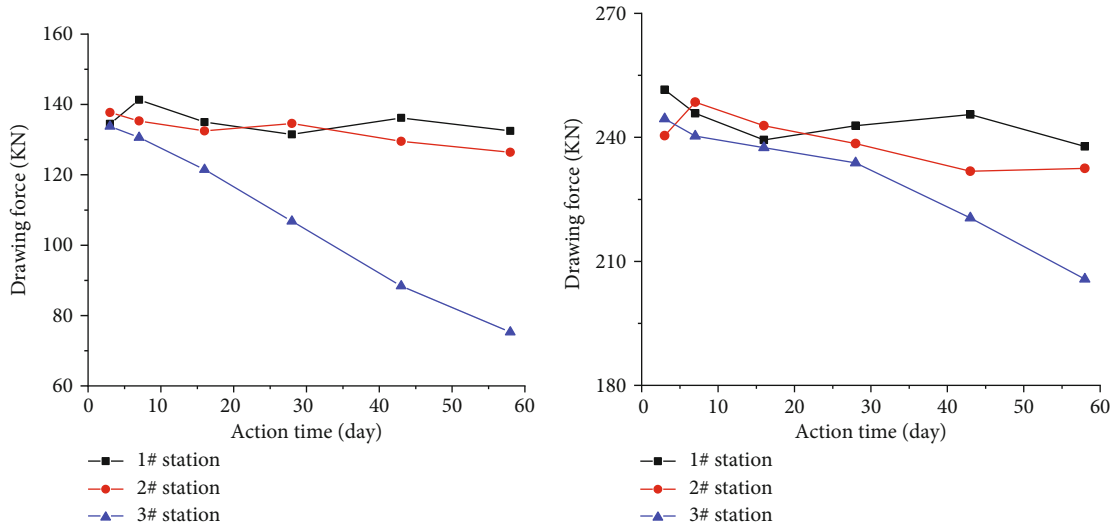

Figure 7: The test results of drawing force with anchor time.

4. Mechanical Response of Anchorage Structures of Weakly Cemented Surrounding Rock with Different Water Contents

The key to improving the anchorage effect is increasing the compressive stress and influence range in the anchorage area [36, 37]. FLAC^{3D} is the numerical calculating software that is applicable for the large deformation of the geotechnical engineering [38]. The model of the anchor structure of a single cable/bolt was built. The bolt and anchor cable were simulated by cable unit. Set different bonding parameters for the anchorage section and the free section of anchor cable, and consider the spreading effect of the tray on the pretightening force. A new rigid connection is established between the anchor cable member and the surrounding rock unit body to simulate the tray after deleting the automatically established connection between the anchor cable member and the surrounding rock. The diameter, length, elastic modulus, and yield strength of the bolt in the model are 20 mm, 2200 mm, 210 GPa, and 500 MPa, respectively. The vertical and horizontal displacements of the lower surface of the model are limited, other surfaces are free boundaries, and the pretightening force is applied at the tail of the anchor.

The distribution laws of the bearing stress, the effective range of compressive stress, and the change rules of anchor axial force are obtained by simulating the influence of water content and anchorage parameters on the prestress diffusion effect of the anchorage structure, combining with the test results of mechanical parameters of weakly cemented rock. According to the conclusions of uniaxial compression test and shear test of weakly cemented rock, as shown in Figures 5 and 6, the functional relationship between the water content of weakly cemented rock and uniaxial compressive strength, elastic modulus, cohesion, and internal friction angle is established, and the functional relationship between the water content of surrounding rock and its deformation parameters and strength parameters is embedded into the numerical model through fish water content, so as to set the water content of surrounding rock of anchor bolt hole.

This is a numerical simulation scheme: (1) when the anchorage length is 0.6 m, the water content of surrounding rocks is 3% and 5%, and the pretightening force of different bolts is 40 kN, 80 kN, 120 kN, and 160kN, respectively; (2) when the pretightening force is 100 kN, the water content of surrounding rocks is 3% and 5%, and the anchor lengths of the bolt are 0.6 m, 0.8 m, 1.0 m, 1.2 m, and 1.4 m, respectively.

4.1. Mechanical Response of Pretension Force to Prestress Diffusion under Different Water Content Conditions. The effective compressive stress area is that the surrounding rock compressive stress is greater than 0.05 MPa in the anchorage structure. The compressive stress is called the effective compressive stress, and the surrounding rock in the effective compressive stress area forms an effective bearing structure. Numerical simulation results under different water contents and pretightening conditions are shown in Figure 8 when the anchorage length is 0.8 m: the effective compressive stress influence area will increase with the increase of the preload force when the surrounding rocks have the same water content. The effective compressive stress is discontinuous when the preload is 40 kN and the water content is 3% and 5%. A continuous effective compressive stress area with a small influence range is formed along the axial direction of the bolt when the preload is increased to 80 kN. The maximum effective range of the effective compressive stress area on the side of the bolt increased from 0.3-0.4 m to 0.6-0.7 m in the process of increasing the preload from 80 kN to 160 kN, and the range of stress areas greater than 0.1 MPa also increased with the preload increase. The higher the water content of the surrounding rock is, the worse the diffusion effect of the preload force is when in the same

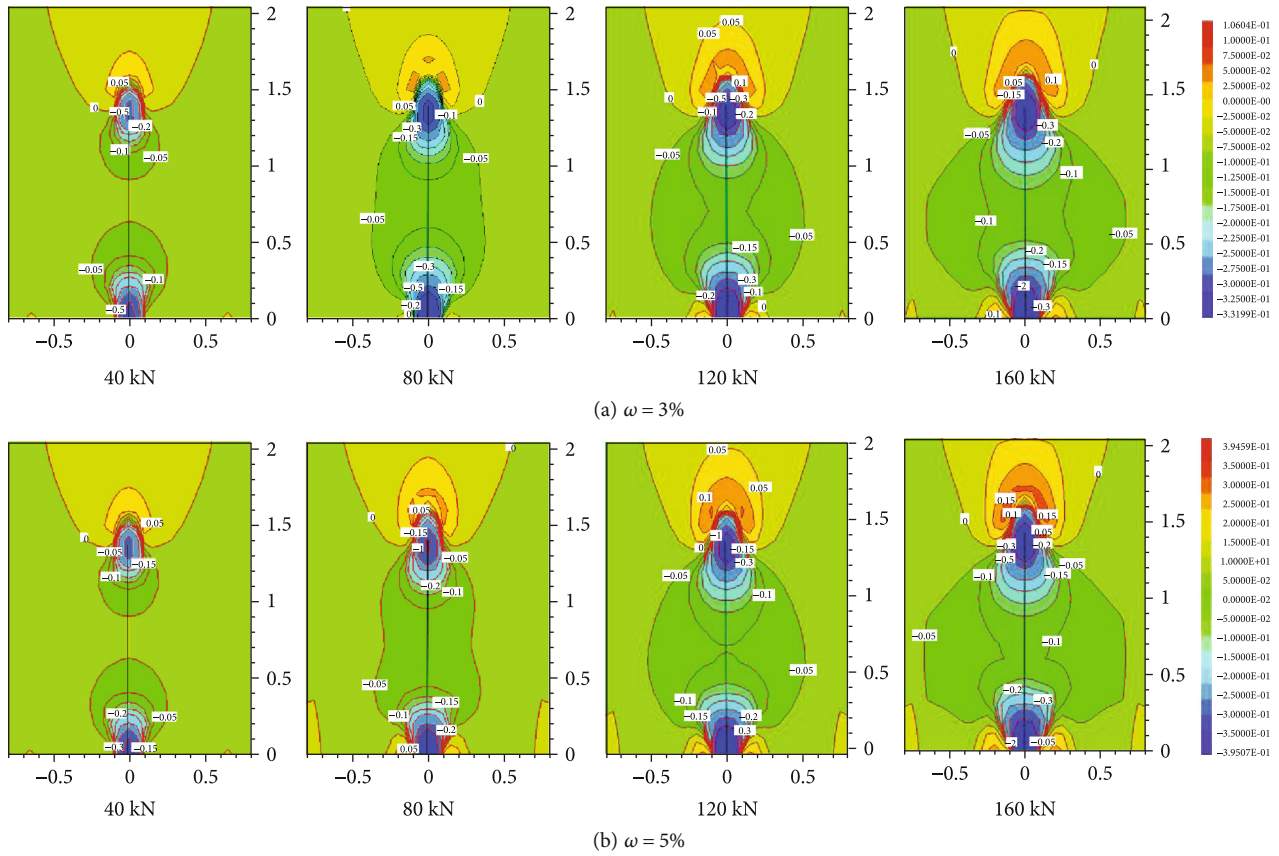

Figure 8: Supporting stress contour in different preloads.

preload. The range of effective compressive stress is reduced slightly, but the range of compressive stress greater than 0.1 MPa is reduced significantly when the water content is increased from 3% to 5%. A high-stress zone greater than 0.1 MPa is formed along the axial direction of the bolt, and the influence range of one side of the bolt is 0.2-0.3 m when the water content is 3%, and the preload reaches 120 kN. However, in order to achieve the same preload diffusion effect, 160 kN preload is required when the moisture content is 5%.

A compressive stress monitoring line is set along the axial direction of the bolt in the center of the model. The free section 0.4-1.0 m away from the tail of the bolt is taken as the research object because the compressive stress is high at the tail of the bolt and the head of the bolt, and the change is not obvious. The change rules of compressive stress under different water contents and preload are shown in Figure 9. The distribution pattern of surrounding compressive stress along the axial direction of the bolt in the free section is the same under different water contents and preloading conditions. The compressive stress will decreases as the water content increases at a distance of 0.4 m from the tail of the bolt. The compressive stress of the surrounding rock in the free section is greater than 0.1 MPa when the water content and preload are 3%, 120 kN, and 160 kN. The compressive stress will be greater than 0.1 MPa after the preload reaches 160 kN when the moisture content is 5%. The stress distribution curves of the water content and preload of 3% and 120 kN are the same as those of the water content and preload of 5% and 160 kN, respectively. Obviously, the higher the water content of the surrounding rock, the worse the diffusion effect of the preload in the surrounding rock.

The variation rules of the axial force of the anchorage section under different water contents and preload is shown in Figure 10. The axial force of the bolt will increase with the increase of the preload when the water content is constant. On the contrary, the axial force of the bolt will decrease with the increase of the water content when the preload is constant. As the anchorage depth increases, the axial force of the bolt decreases rapidly but the axial force of the bolt is close to 0 when the water content and the anchorage depth are 3% and 0.2 m and 5% and 0.3 m, respectively. Obviously, reducing preload and increasing water content of surrounding rock can weaken the diffusion effect of prestress in surrounding rock because the increase of the water content makes the longer anchorage section subject to the tensile force of the bolt and the performance of the anchor agent decreases with the increase of the water content.

Obviously, the increase of the water content of the surrounding rock is bad for the diffusion of the prestress in the surrounding rock. The higher the water content of the surrounding rock, the more difficult is to exert the constraining effect of the prestress on the surrounding rock, and it is more difficult to form an effective anchored bearing structure. Therefore, the prestress should be increased to avoid the attenuation of the prestress diffusion effect caused by

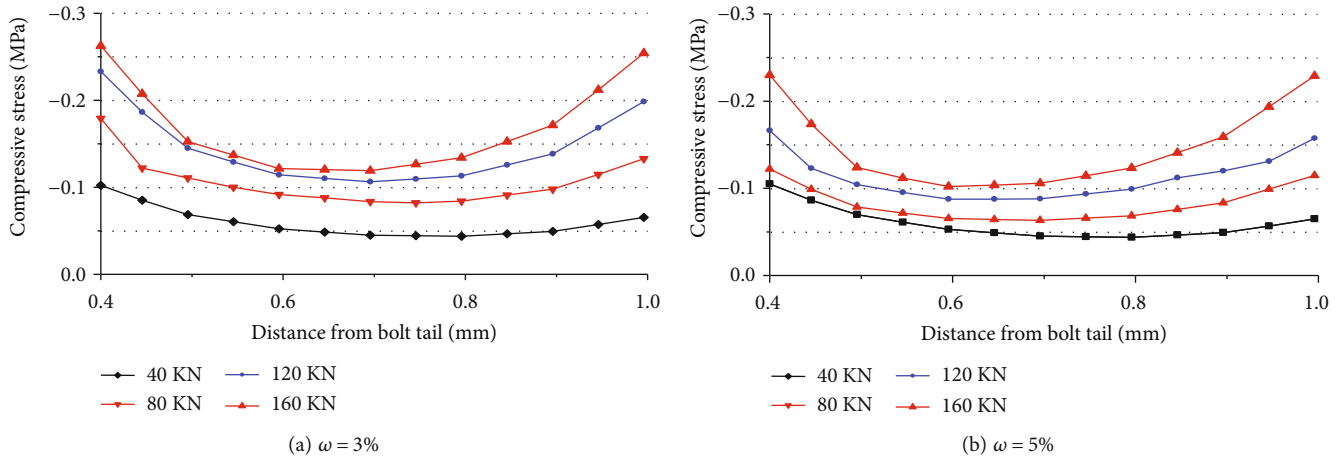

Figure 9: Distribution curve of compressive stress along the bolt axis direction.

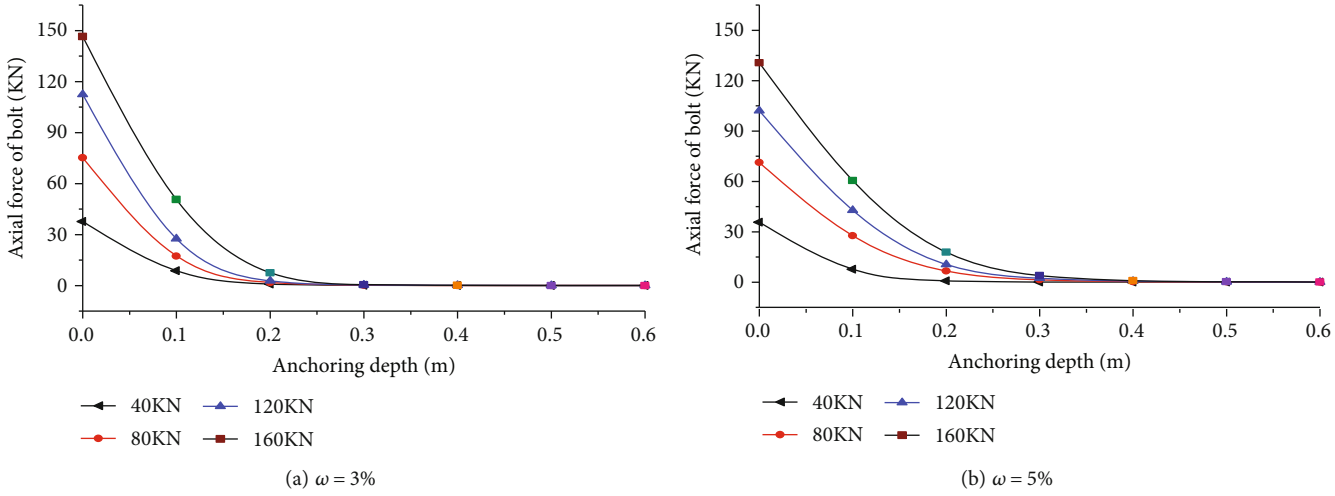

Figure 10: Variation curve of axial force of anchorage section.

the water, to decrease the influence of the increase of water content on the preload diffusion, and to ensure the reliability of the anchorage structure under the condition that the surrounding rock contains water.

4.2. Mechanical Response of Anchorage Length to Prestress Diffusion with Different Water Contents. The distribution laws of the support stress and the range of effective compressive stress are shown in Figure 11 under different water contents and anchor length conditions, and the prestress of the bolt is 120 kN. When the water content is constant, as the length of the anchorage increases, the range of effective compressive stress decreases gradually, but the value of compressive stress increases gradually. The maximum influence range of compressive stress greater than 0.1 MPa on the side of the bolt will reach 0.3 m when the anchorage length is 0.8 m and the water content is 3%. But a continuous area has not formed with compressive stress greater than 0.1 MPa along the axial direction of the bolt when the water content is 5%. The difference in compressive stress distribution is reduced significantly between 3% and 5% water content when the anchorage length is 1.4 m. As the water content increases, the effective compressive stress and the influence range will decrease when the anchorage length is constant. Apparently, the longer the anchorage length, the smaller the influence range of the water content change on the compressive stress in surrounding rock.

The change of compressive stress under different water contents and anchor length conditions is shown in Figure 12: the distribution of compressive stress along the axial direction of the anchor rock of the free section is the same under different water contents and anchor lengths, and the maximum compressive stress decreases significantly with the increase of the water content. The compressive stress of each anchorage length at 0.2 m from the tail of the bolt is 1.4-1.6 MPa when the water content is 3%, and the compressive stress is 0.9-1.1 MPa when the water content is 5%. The higher the water content, the smaller the range of compressive stress. The positions of compressive stress greater than 0.2 MPa in the model are 0.7 m and

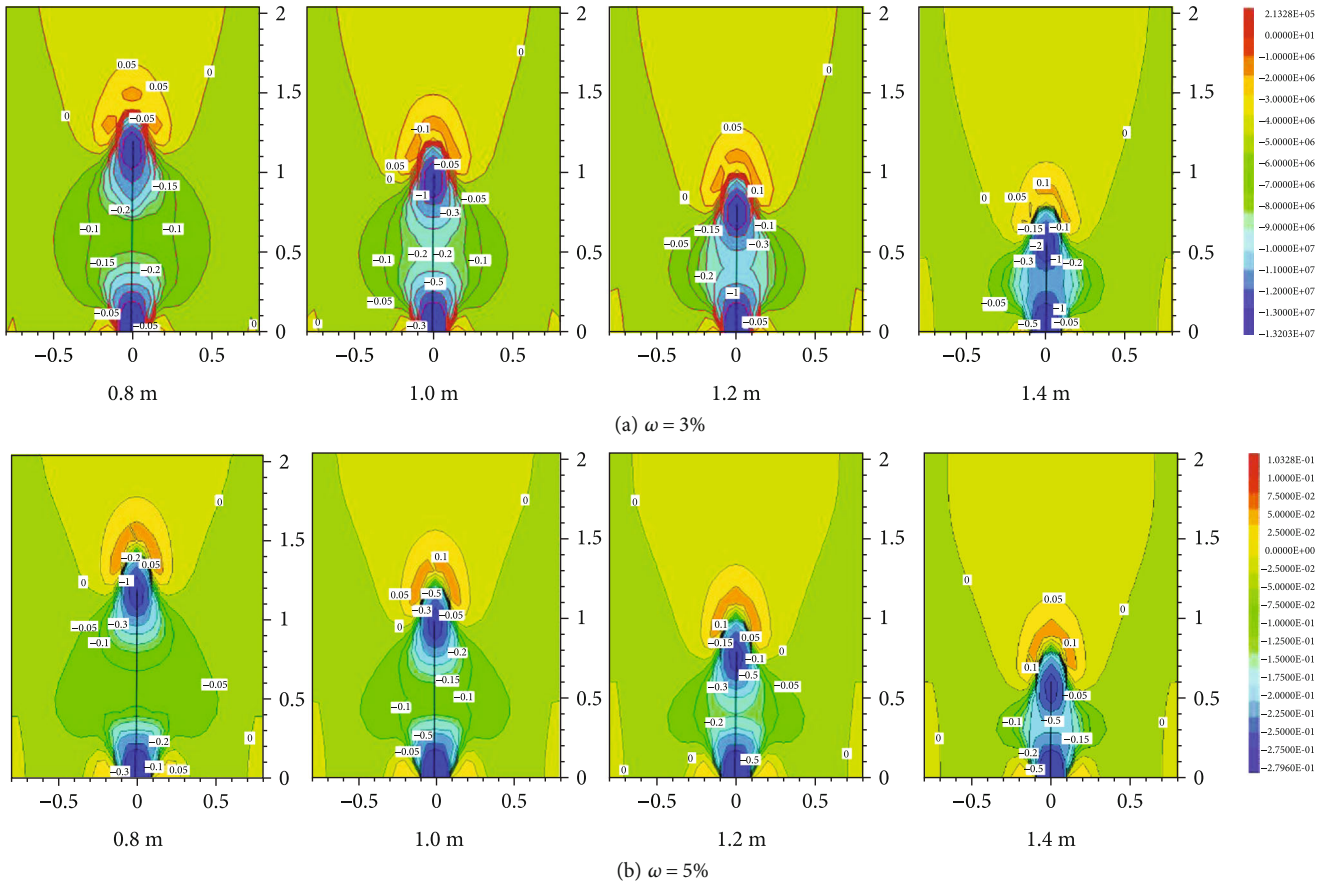

Figure 11: Supporting stress contour in different anchorage lengths.

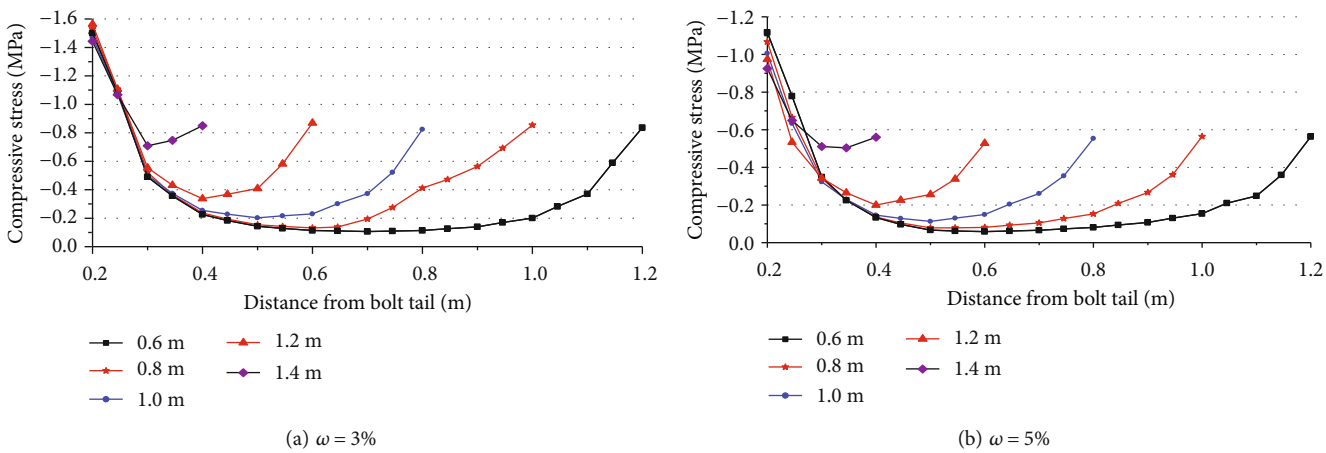

Figure 12: Distribution curve of axial direction compressive stress.

0.85 m from the tail of the bolt when the anchorage length is 0.8 m and the water content is 3% and 5%, and increasing the anchoring length of the bolt can increase the surrounding rock compressive stress with the increase of water content.

Apparently, the range of higher compressive stress in the surrounding rock and compressive stress will increase when lengthening the anchorage section. However, the increase of anchorage length will reduce the range of effective compressive stress, which is bad for the spread of prestress in surrounding rocks. Therefore, the length of the anchoring section should be appropriately lengthened, so that a large range of high-pressure stress zones can be formed in the surrounding rock, and a certain length of the free section is reserved to obtain a larger influence range of effective compressive stress for anchoring in

water-containing surrounding rocks. In addition, the methods are to be improved the preload of the bolt, ensured the diffusion effect of the preload in the surrounding rock, and increased the reliability of the anchoring structure.

5. Conclusion

(1) The sandy mudstone is the main component of the No. 1802 tailentry immediate roof, and there is a conglomerate coarse sandstone aquifer above the immediate roof. The aquifer is relatively close to the entry and unstable. The average distance between the aquifer and the entry is 3.13 m. When the aquifer horizons are low, the excavation of the entry caused the cracks to develop in the weakly cemented rock layer of the immediate roof, which provided the channels for the water flowing on the roof. It is the key reason for the collapse of No. 1802 tailentry surrounding rock

(2) Kaolinite and chlorite are the main clay minerals in weakly cemented rocks with contents of 33.1% and 21.6%. They have strong water absorption properties and easy weathering characteristics. The softening coefficient of weakly cemented rock is 0.082. The relationship between ω and σ, E, c, and φ of weakly cemented rocks was obtained based on uniaxial compression and shear experiments. ω decreases exponentially with σ and E, and it decreases linearly with c and φ

(3) The increase of the water content of the surrounding rock is damaged for the diffusion of the preload in the surrounding rock. The higher the water content of the surrounding rock, the smaller the diffusion range of the preload. It can avoid weakening its diffusion effect due to the action of water and ensures the diffusion effect of the preload in the surrounding rock

(4) The reliability of the anchoring structure can avoid weakening its diffusion effect due to the action of water and make up for the influence of increased water content on the preload diffusion. Lengthening the anchorage section can increase the stress of the surrounding rock. And the increase of the anchoring length will reduce the effective range of effective compressive stress, which is damaged for the spread of preload in the surrounding rock

Data Availability

The data used to support the findings of this study are available from the corresponding author upon request.

Conflicts of Interest

The authors declare that there are no conflicts of interest.

Acknowledgments

This work is supported by the Natural Science Foundation of Xinjiang Uygur Autonomous Region (2022D01A52; 2020D01A45; 2021D01B34), National Natural Science Foundation of China (52074239), Young Doctoral Science and Technology Talents of Xinjiang (2020Q080), and Doctoral Initiation Fund of Xinjiang Institute of Engineering (2019BQJ012207).

References

[1] H. Y. Fu, G. K. Zhou, and L. Zeng, "Study on slaking particle distribution characteristics of carbonaceous mudstone," *Applied Mechanics & Materials*, vol. 170, pp. 352–356, 2012.

[2] H. Yamaguchi, K. Yoshida, I. Kuroshima, and M. Fukuda, "Slaking properties of mudstone," *Soil Mechanics & Foundation Engineering*, no. 406, pp. 17–26, 1989.

[3] J. Hadizadeh and R. D. Law, "Water-weakening of sandstone and quartzite deformed at various stress and strain rates," *International Journal of Rock Mechanics and Mining Sciences & Geomechanics*, vol. 28, no. 5, pp. 431–439, 1991.

[4] P. Rajeev and J. Kodikara, "Numerical analysis of an experimental pipe buried in swelling soil," *Computers and Geotechnics*, vol. 38, no. 7, pp. 897–904, 2011.

[5] G. Fan, M. Chen, D. Zhang et al., "Experimental study on the permeability of weakly cemented rock under different stress states in triaxial compression tests," *Geofluids*, vol. 2018, 9 pages, 2018.

[6] T. T. Lin, C. Sheu, J. E. Chang, and C. H. Cheng, "Slaking mechanisms of mudstone liner immersed in water," *Journal of Hazardous Materials*, vol. 58, no. 1-3, pp. 261–273, 1998.

[7] J. Qi, W. Sui, Y. Liu, and D. Zhang, "Slaking process and mechanisms under static wetting and drying cycles slaking tests in a red strata mudstone," *Geotechnical & Geological Engineering*, vol. 33, no. 4, pp. 959–972, 2015.

[8] H. J. Mao, C. H. Yang, X. L. Huang, and X. C. Wang, "Experimental study and theoretical analysis of slates under different saturated conditions," *Rock and Soil Mechanics*, vol. 43, no. 9, pp. 1637–1642, 2006.

[9] S. Y. Wen, J. Li, X. Su, and X. Yao, "Studies of mesomechanical structure characters of surrounding rock failure under complex stress state," *Rock and Soil Mechanics*, vol. 31, no. 8, 2010.

[10] X. R. Ge, "Deformation control law of rock fatigue failure, real-time X-ray CT scan of geotechnical testing, and new method of stability analysis of slopes and dam foundation," *Chinese Journal of Geotechnical Engineering*, vol. 30, no. 1, pp. 1–20, 2008.

[11] Y. P. Li, L. Z. Chen, and Y. H. Wang, "Experimental research on pre-cracked marble under compression," *International Journal of Solids and Structures*, vol. 42, no. 9-10, pp. 2505–2516, 2005.

[12] M. Prudencio and M. Van Sint Jan, "Strength and failure modes of rock mass models with non-persistent joints," *International Journal of Rock Mechanics & Mining Sciences*, vol. 44, no. 6, pp. 890–902, 2007.

[13] C. A. Tang and S. Q. Kou, "Crack propagation and coalescence in brittle materials under compression," *Engineering Fracture Mechanics*, vol. 61, no. 3-4, pp. 311–324, 1998.

[14] A. Munjiza, *The Combined Finite-Discrete Element Method*, Wiley, Chichester, 2004.

[15] W. M. Wang, J. C. Sun, and L. X. Lv, "Study of in-situ stress inversion in weakly consolidated soft rock based on damped least square method," *Journal of China University of Mining & Technology*, vol. 5, pp. 34–37, 2004.

[16] W. M. Wang, Z. H. Zhao, and L. Wang, "Elastic-plastic damage analysis for weakly consolidated surrounding rock regarding stiffness and strength cracking," *Journal of Mining & Safety Engineering*, vol. 30, no. 5, pp. 679–689, 2013.

[17] Z. Y. Song, H. G. Ji, Y. J. Liu, and L. H. Sun, "Influencing factors of excavation disturbance on neighboring roadways in weakly cemented rock," *Journal of Mining & Safety Engineering*, vol. 33, no. 5, pp. 806–812, 2016.

[18] Q. B. Meng, L. J. Han, W. G. Qiao, D. G. Lin, and J. D. Fan, "Evolution of surrounding rock in pioneering roadway with very weakly cemented strata through monitoring and analysing," *Journal of China Coal Society*, vol. 38, no. 4, pp. 572–579, 2013.

[19] Q. B. Meng, L. J. Han, W. G. Qiao, J. Zhang, F. Q. Mei, and W. Feng, "Supporting effect and application of bolt-net-anchor coupling support under extremely weak cementation formation," *Journal of Mining & Safety Engineering*, vol. 33, no. 5, pp. 770–778, 2016.

[20] Q. B. Meng, L. J. Han, and H. Pu, "Research and monitoring analysis of coal roadway bolting system in very weakly cemented stratum," *Journal of China Coal Society*, vol. 41, no. 1, pp. 234–245, 2016.

[21] Q. B. Meng, L. J. Han, and W. G. Qiao, "Elastic-plastic analysis of the very weakly cemented surrounding rock considering characteristics of strain softening and expansion," *Journal of China University of Mining & Technology*, vol. 47, no. 4, pp. 760–767, 2018.

[22] Q. B. Meng, L. J. Han, W. G. Qiao, D. G. Lin, S. Y. Wen, and J. Zhang, "Deformation failure characteristics and mechanism analysis of muddy weakly cemented soft rock roadway," *Journal of Mining & Safety Engineering*, vol. 33, no. 6, pp. 1014–1022, 2016.

[23] Y. B. Wang, J. D. Jing, D. Q. Zhang, and S. L. Jiang, "Technology of control deformation and failure of weakly consolidated soft-rock roadway and its application," *Coal Mine and Technology*, vol. 19, no. 2, pp. 53–57, 2014.

[24] G. l. He, W. M. Wang, W.-S. Zhang, and X. Z. Lv, "Study on cross-section form and support optimization in weakly consolidated soft rock roadway," *Coal Engineering*, vol. 49, no. 1, pp. 38–41, 2017.

[25] Q. Bai and S. Tu, "Failure analysis of a large span longwall drift under water-rich roofs and its control techniques," *Engineering Failure Analysis*, vol. 67, pp. 15–32, 2016.

[26] J. Sun and X. Qian, "Analysis of coal mine accidents in China during 2004-2015," *Ind. Mine Automat*, vol. 42, pp. 1–5, 2016.

[27] Q. H. Wu, C. L. Xie, Y. S. Xie et al., "Extending application of asymmetric semi-circular bend specimen to investigate mixed mode I/II fracture behavior of granite," *Journal of Central South University*, vol. 29, no. 4, pp. 1289–1304, 2022.

[28] L. Weng, Q. H. Wu, Y. L. Zhao, and S. M. Wang, "Dynamic response and failure of rock in initial gradient stress field under stress wave loading," *Journal of Central South University*, vol. 27, no. 3, pp. 963–972, 2020.

[29] H. Bokar, A. Z. Traoré, A. Mariko et al., "Geogenic influence and impact of mining activities on water soil and plants in surrounding areas of Morila Mine, Mali," *Mali. Journal of Geochemical Exploration*, vol. 209, p. 106429, 2020.

[30] Q. W. Zhu, H. Li, and X. H. Yang, "Influence analysis of between subsidence and structure evolution in overburden rock under mining," *Journal of China Coal Society*, vol. 57, 2019.

[31] C. H. Yang, H. J. Mao, X. C. Wang, X. H. Li, and J. W. Chen, "Study on the variation on microstructure and mechanical properties of water-weakening slates," *Rock and Soil Mechanics*, vol. 27, no. 6, pp. 2090–2098, 2006.

[32] S. B. Li, J. Chen, and G. D. Yi, "Experimental study on the relationship between micro- characteristics and compressive strength of the red bed rock," *Geotechnical Investigation & Surveying*, vol. 41, no. 3, pp. 1–5, 2013.

[33] X. Shi, Y. F. Cheng, S. Jiang, D. S. Cai, and T. Zhang, "Experimental study of microstructure and rock properties of shale samples," *Chinese Journal of Rock Mechanics and Engineering*, vol. 33, Suppl 2, pp. 3439–3445, 2014.

[34] A. V. Dyskin, E. Sahouryeh, R. J. Jewell, H. Joer, and K. B. Ustinov, "Influence of shape and locations of initial 3-D cracks on their growth in uniaxial compression," *Engineering Fracture Mechanics*, vol. 70, no. 15, pp. 2115–2136, 2003.

[35] H. Lee and S. Jeon, "An experimental and numerical study of fracture coalescence in pre-cracked specimens under uniaxial compression," *International Journal of Solids and Structures*, vol. 48, no. 6, pp. 979–999, 2011.

[36] H. P. Kang, J. H. Wang, and J. Lin, "Case studies of rock bolting in coal mine roadways," *Chinese Journal of Rock Mechanics and Engineering*, vol. 29, no. 4, pp. 649–664, 2010.

[37] R. Wang, J. B. Bai, S. Yan, Y. B. Song, and G. D. Wang, "An improved numerical simulation approach for the failure of rock bolts subjected to tensile load in deep roadway," *Geofluids*, vol. 2020, 21 pages, 2020.

[38] F. Itasca and Itasca Consulting Group Inc, "Fast language analysis of continua in 3 dimensions," *Online Manual*, 2013.